## Disinfection Robots Scheduling and Routing Problem for Healthy Buildings

Ziwei Liu<sup>a</sup>, Yifang Xu<sup>b</sup>, Mingzhou Jin<sup>a, \*</sup>, Shuai Li<sup>b</sup>

- a. Industrial and Systems Engineering, University of Tennessee, Knoxville, TN, 37996, USA
  - b. Civil Engineering, University of Tennessee, Knoxville, TN, 37996, USA

#### **Abstract**

Disinfection robots have been developed and deployed to maintain the environmental hygiene of built environments. Given the dynamic activities and varying infection risks within these environments, as well as the limited number of disinfection robots in buildings, optimizing their scheduling and routing is critical to achieve the full potential of automated disinfection and cleaning in buildings. Therefore, this research proposed a new model and method to minimize the infection risk. Specifically, the study used an improved fomite-based pathogen transmission model to assess the varying infection risks associated with the operational schedules and human activities. Based on the team orienteering problem and vehicle routing problem with time windows, a mixed-integer programming model was developed to optimize robot disinfection schedules and routes to mitigate the overall infection risk within a building. Numerical experiments were conducted to evaluate the proposed method, demonstrating that the mixed-integer programming was effective in solving the optimization problem for buildings with less than 50 rooms. A real case study based on a campus building was also conducted to demonstrate the applicability of the proposed method. Different pathogens were introduced, and the impacts of the disinfection robot speed parameter and the number of robots on risk reduction were also evaluated through sensitivity analyses. This study has shown great potential to reduce the exposure risks of building occupants to infectious diseases and eliminate hotspots of community transmissions. This research could be scalable and adaptable to facilities with different functions, configurations, and sizes.

**Keywords:** Built Environment; Pathogen Transmission; Health; Infection Risk; Disinfection Robot Scheduling

## 1. Introduction

The COVID-19 pandemic swept the world for nearly three years, unleashing unprecedented shocks to society and household life [1], leading to heavy burdens on healthcare systems, and disrupting education and the economy [2,3]. The SARS-CoV-2 is not the first and will not be the last pathogen that causes pandemics and such disastrous consequences. In developed nations, people spend about 90% of their time in built environments, encompassing all facets of our lives [4]. Airborne pathogens such as SARS-CoV-2 and influenza spread quickly in enclosed built environments [5,6], making buildings hotspots for nightmarish infections. The entire world has sought new measures to curb the spread of infectious diseases. Disinfection and cleaning are important practices to mitigate the spread of infectious

E-mail address: jin@utk.edu (M. Jin).

<sup>\*</sup> Corresponding author.

pathogens in mass-gathering built environments, such as healthcare facilities, commercial buildings, airports, and schools [7]. The COVID-19 virus may persist on inorganic surfaces for many days or weeks [8], which may cause a healthy person to get infected in addition to human-to-human proximity contact transmission. Currently, most of the indoor disinfection in contaminated areas were performed by human workers using chemical disinfectants [7]. However, manual disinfection is time-consuming and labor-intensive. It also increases the chance of a healthy human becoming exposed to the highly contagious virus, particularly when personal protective equipment is not properly worn or is missing. Moreover, consistent procedures cannot be guaranteed for the required level of disinfection and cleaning.

There is a critical need for automated, intelligent, and precision disinfection to reduce pathogen transmission and exposure and thus prevent outbreaks of infectious diseases. Autonomous or remotecontrolled disinfection robots could provide safe, fast, and effective disinfection. During the pandemic, robot-controlled noncontact ultraviolet (UV) surface disinfection have been deployed in many facilities to clean and disinfect contaminated surfaces[9]. The elevated concerns driven by the pandemic of COVID-19 have increased the adoption of robotic technology for infection control and environmental hygiene, providing a massive impetus to the market of disinfection robots. However, there are two unaddressed technical challenges preventing the effective deployment of disinfection robots in massgathering facilities to maintain environmental hygiene and public health. First, varying schedules and dynamic human activities in the rooms of a building significantly affects the accumulation of pathogens on room surfaces and thus impact the infection risks [10]. Existing disinfection robots and decision support systems are unable to compute the infection risks and exploit the infection risks to plan and optimize disinfection robot scheduling and routing. Optimized robot scheduling and routing is the key to achieving automated and effective cleaning and disinfection. Second, given the limited number of available disinfection robots and the spaces needing disinfection, there lacks an optimization model to simultaneously plan robot schedules and routes to minimize the infection risks while not disrupting the on-going human activities in buildings.

To address the technical challenges, this research exploited an improved fomite-based transmission model to assess the infection risks at the room level based on the planned schedule, human activities, and building characteristics. Then, based on the team orienteering problem and vehicle routing problem with time windows, we developed a mixed-integer programming model to optimize robot disinfection schedules and routes to mitigate the overall infection risk within the building. The rest of the paper is organized as follows. Relevant studies are reviewed in Section 2 to identify the knowledge gaps and technical barriers. Section 3 describes the proposed method and the decision support system and provides numerical experiments with randomly generated instances. Section 4 presents a real case study based on a building at the University of Tennessee to demonstrate the application of the developed

models. In Section 5, we discuss the applicability and scalability, list the limitations and future research directions, and conclude the study with major findings.

#### 2. Literature Review

## 2.1 Building disinfecting

Several studies have demonstrated that fomites can be an essential route to the spread of SARS-CoV-2 [11–13]. Fomites, referring to contaminated objects or surfaces, can be contaminated by an infected host by excretion behaviors such as coughing and sneezing. The respiratory particles can be expelled onto hands, which then touch a surface, or directly fall to the surface. An individual may touch contaminated objects, transfer the infectious particles from fomites to the susceptible sites (e.g., facial mucosa), and get inoculated [14]. Laboratory studies indicated that the SARS-CoV-2 virus can persist a long time on surfaces [15]. Furthermore, recent studies found that SARS-CoV-2 RNA has been found on surfaces in different facilities, such as restaurants, grocery stores, and healthcare settings [16,17], indicating that fomite transmission is an important route in indoor environments. To assess the pathogen transmission via the fomite route, the environmental infection transmission system (EITS) modeling framework has been developed to model the pathogen transmission pathway. The framework divides the individuals as susceptible (S), infectious (I), and removed (R), and considers the dynamics of inoculation of S, pathogen transmission between hands and fomites for I, S, and R, excretion activities performed by I, pathogen decay in the environment, recovery of I [18], and cleaning events.

The potential SARS-CoV-2 outbreak caused by fomite transmission in indoor environments calls for a need for implementing mitigation measures to control the transmission risk and maintain a healthy indoor environment. Surface disinfection has been proven to be effective to curb fomite-mediated transmission. For instance, chemical disinfectants, such as bleach and ethanol, can be used as sanitizer for surface cleaning, and mass spray chemical disinfection has already been adopted via artificial intelligence such as robots and unmanned vehicles [11]. Disinfection robots, as a promising tool for indoor surface cleaning during the pandemic [19], are adopted to disinfect the building surfaces in this study.

Predicting outbreak risks in buildings considering the building-specific characteristics is challenging. First, building structure could influence indoor microbial communities. The distribution of microbiomes in rooms with different configurations and functionalities is considerably different [20,21]. Second, occupancy could significantly influence microbial distribution patterns. For instance, the bacterial communities in rooms with high occupant diversity exhibit differences from the rooms with low occupant diversity [22]. The microbial exchange occurs between occupants and contaminated surfaces. The outbreak risks could vary significantly for rooms with different functionalities and different occupancy levels. For a single room with changes of occupancy and disinfection schedules, the outbreak

risk varies according to the room operation schedule during a day. However, there lacks a computational modeling framework integrating the building-specific information, room operational schedule (e.g., occupancy schedule and disinfection schedule), and pathogen transmission to assess the time-varying room infection risk. Therefore, it is essential to develop a computational framework to analyze the infection risks influenced by temporal factors, such as the change of occupancy and disinfection, and spatial factors, such as spatial configurations of rooms.

### 2.2 Optimization for disinfecting scheduling and routing

Coexisting with various viruses and bacteria is a global reality that comes with unique challenges impacting daily interactions [23]. Many organizations have paid attention to the development of disinfection robots [23-25], and numerous optimizations focusing on avoiding obstacles and navigation for disinfection robots [27,28]. Research seldom focused on the schedule optimization problem of disinfection robots. However, it is impossible for the facility to have unlimited robots considering the high cost of robots. This study aims to solve the schedule optimization problem of disinfection robot based on time windows. Our optimization model integrates facets of the Team Orienteering Problem (TOP) with the complexities inherent in time window constraints and network flow dynamics. The objective is to mitigate as much risk as possible. Therefore, the following literature reviews mainly focus on the TOP and their applications.

Vehicle routing problems (VRPs) are among the most studied problems in the area of combinatorial optimization [29]. The orienteering problem (OP) is one of the variants of VRP, which can be seen as a combination of node selection, determining the shortest Hamiltonian path of the selected nodes, and maximizing the total score collected from selected nodes. There are two review papers that introduce the general orienteering problems in detail [30,31]. Most recent research on the orienteering problem with profits assumes that the profit collected at each vertex is a fixed value, such as the TOP, in which multiple routes need to be determined to maximize the total profits within a given time budget [32,33], the team orienteering problem with time window (TOPTW), in which each vertex can only be visited within a given time window [33-38], and the time dependent orienteering problem (possibly with time window), in which the traveling time between two vertices is time-dependent [39-41]. In another study, TOP with Variable Profits (TOPVP) was examined [43]. The distinguishing feature of this problem is that the total score of visiting a vertex depends on the time duration of the visit, with no relevance given to the temporal specificity of the visitation. The Multi-objective TOP with Time Windows was proposed by [44], in which each POI has several profits, and the objective function of the problem maximizes a profit vector instead of a scalar quantity. The TOP with Time Windows and Time-Dependent Scores (TOPTWTDS) was also investigated by [45] to consider time-dependent scores. The TOP with Time-Varying Profit considered the situation when arrival time and service time affect the collection of profits [46].

VRPTW adds a time window constraint of VRP, which means that a vehicle must begin its service inside a time window at a demand point. For more models, the classification and solving algorithms of VRP and its variants, we suggest two latest review papers [29] and [47]. The biggest difference of our schedule optimization problem of disinfection robots from TOP and VRPTW is (1) the profit (risk) in our problem serves as a variable not a parameter, contingent on the timing of the node visit; (2) the same node may be visited multiple times, each occurring within a distinct time window, and (3) the objective is to mitigate as much risk for all occupants as possible under the schedule and resource restriction.

### 3. Decision support system for disinfecting rooms

#### 3.1 Support system framework

To assess room infection risks, the parameters required in the fomite-based pathogen transmission model includes the room environmental parameters, occupant characteristics, disinfection information, and pathogen-specific parameters. Figure 1 indicates the required information for infection risk assessment. To acquire the environmental parameters, BIM was used to automatically extract the room characteristics (e.g., the accessible surface). The occupant characteristics were retrieved from the room schedule. The information of the room schedule includes the number of times a room is occupied or empty for a day, the duration of each occupation, and the number of occupants during each occupation. Therefore, the occupant characteristics were expressed as temporal varying parameters according to the room schedule. In this study, it is considered that a room can be disinfected when the room is unoccupied. At each unoccupied time, the disinfection is a binary variable representing whether the room is being disinfected or not. As a focus on the potential COVID-19 outbreak, the pathogen-specific parameters regarding the SARS-CoV-2 were used in the pathogen transmission model.

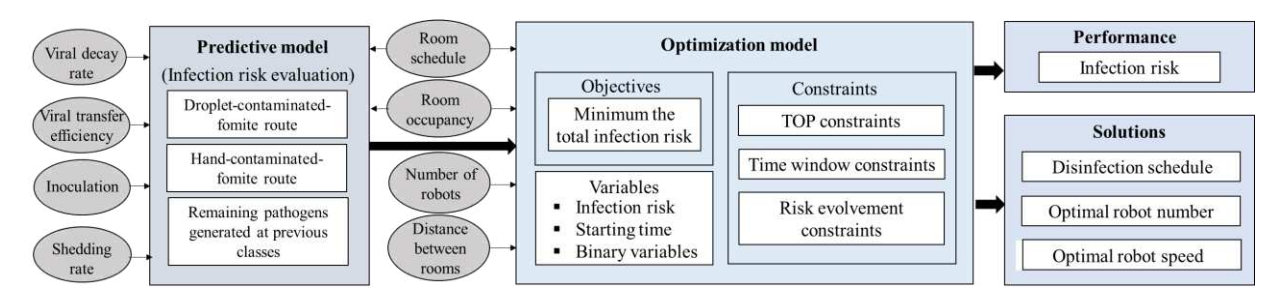


Figure 1. Overall support system framework.

## 3.2 Fomite-based pathogen transmission model

Fomites are defined as surfaces accessible to human hands. A surface can be contaminated in two ways:

1) droplets excreted from coughing, sneezing, or exhaling by an infector that deposits to the surface; 2) touching by contaminated hands. The hands of a susceptible person are contaminated with pathogens via fomite touching, and the pathogens on the hands may be inoculated by the susceptible person when the person touches the mouth or other mucous membranes. The Environmental Infection Transmission

System (EITS) modeling framework describes the dynamics of pathogen persistence on surfaces and hands, and the dynamics of hand contact and pathogen transmission. The EITS framework considers that each individual is either susceptible (S), infected (I), or immune (R). Pathogens excreted from an I individual are either deposited on fomites (F) or the hands of I ( $H_I$ ) which may further transfer to F via hand-touching activities. Pathogens surviving on F may transfer to hands of individuals S and R ( $H_S$ ,  $H_R$ ) via fomite touching behavior. An S individual may get infected by inoculating pathogens on  $H_S$ . The dynamic process is modeled using equation (1-3) [18,48].

$$P_{inoc} = \frac{\rho \chi}{\mu_H + \rho_{HF} + \rho \chi} \tag{1}$$

$$P_{dep} = \frac{\rho_{HF}}{\mu_H + \rho_{HF} + \rho \chi} \tag{2}$$

$$P_{pick} = \frac{\frac{M\rho_{FH}}{M\rho_{FH} + \mu_{F}}}{1 - \frac{M\rho_{FH}}{(M\rho_{FH} + \mu_{F})} \frac{\rho_{HF}}{(\mu_{H} + \rho_{HF} + \rho_{\chi})}}$$
(3)

where  $P_{inoc}$  is the proportion of pathogens that survive on hands and being inoculated by a susceptible person;  $P_{dep}$  is the proportion of pathogens transfer from hands to fomites;  $P_{pick}$  is the proportion of pathogens picked up from fomites to hands, and the equation describes the infinite sequence of pickup and redeposition process. M is the population size, or occupancy size,  $\rho$  is the inoculation rate,  $\mu_H$  is the viral decay rate on hands,  $\mu_F$  is the viral decay rate on fomites,  $\rho_{HF}$  is the transfer efficiency from hands to fomites,  $\rho_{FH}$  is the transfer efficiency from fomites to hands, and  $\chi$  is the proportion of pathogens absorbed during self-inoculation.

This model particularly fits for places like school buildings and classrooms, where individuals frequently interact with surfaces (e.g., hands and desks), a fomite-based approach is contextually relevant. Leveraging the well-established Environmental Infection Transmission System (EITS) modeling framework, known for its effectiveness in addressing fomite transmission issues, we chose to enhance this model specifically for school building scenarios. This choice enables us to understand the impact of interventions like surface cleaning scheduling on reducing transmission risks.

# 3.3 Optimization modeling and solution method

Consider the scheduling problem of disinfecting a set of rooms, N, with robots within T time windows. Each room  $i \in N$  has  $w_i$  time windows in which a robot can disinfect it. To facilitate modeling, we define an augmented graph G = (V, E), where V is the set of nodes and E is the set of edges. Each node or class in V is featured by a duplex of room and time window, (i, t), where  $i \in N$  and  $t \in \{1, ..., T\}$ . We let  $V_i \subseteq V$  be the subset of nodes that are associated with room i but have different time windows.

 $|V| = 1 + \sum_{i \in N} w_i$ . Node u is called a precedent node to v (i.e, u = prec(v)) if they both correspond to the same room but node v has a time window immediately after u. E is the set of all valid edges that connect nodes u to v such that the time window of v is not earlier than that of u. Variable  $r_u$  represents the risk of the room associated with the node at the end of the corresponding time window. For a node u = (i, t),  $c_u = \sum_{q=t+1}^{t'-1} M_{iq}$  where t' is the next available time window of room i after t,  $M_{iq}$  is the occupancy at room i in time window q.  $B_u$  is the change of risk between node u = (i, t) and prec(u).

Let  $S_u$  be starting time of node u, if served.  $f_u$  is the cleaning time concerning node u.  $[L_u, U_u]$  is the time window of each node, during which disinfecting can be done at the corresponding room. The following mixed integer program (MIP) determines the optimal disinfecting schedule to minimize the total infection risk of all occupants. Binary variable  $x_{uvk}$  is equal to 1 if robot k travel from node k to disinfect node k; and binary variable k0 is equal to 1 if node k1 is served.

$$\min \sum_{u \in V} c_u r_u \tag{4}$$

s.t

$$\sum_{v \in V} \sum_{k \in K} x_{uvk} = y_v \qquad \forall v \in V/\{0\}, \tag{5}$$

$$\sum_{v \in V} x_{0vk} = \sum_{v \in V} x_{v0k} \le 1 \qquad k \in K, \tag{6}$$

$$\sum_{u \in V} x_{uvk} = \sum_{u \in V} x_{vuk} \qquad \forall k \in K, \forall v \in V/\{0\}, \tag{7}$$

$$S_u + t_{uv} + f_u - S_v \le M(1 - \sum_{k \in K} x_{uvk}) \qquad u \in V, (u, v) \in E,$$
 (8)

$$L_u y_u \le S_u \tag{9}$$

$$S_u + f_u \le U_u y_u \qquad \forall u \in V \,, \tag{10}$$

$$r_u \ge r_{prec(u)} + B_u - My_u \qquad u \in V, \tag{11}$$

$$r_u \le M(1 - y_u) \qquad \qquad u \in V, \tag{12}$$

$$x_{uvk}, y_u \in \{0,1\}; S_u, r_u, r_{prec(u)} \ge 0.$$
 (13)

Objective function (4) minimizes the total risks of all occupants at all nodes. Constraint set (5) decides the value of  $y_v$  and ensures a node can be disinfected at most once. Constraint set (6) ensures robots go out from the depot and return to the depot after finishing all disinfection tasks. The inequality of the left side of constraint set (6) means the robot can only go to at most one place. Constraint set (7) ensures conservation at all nodes except the depot. Constraint sets (8-10) related to the starting time and time

window of each node, which are time constraints for the robots' room cleaning schedules. Constraint sets (11) and (12) represent the risk evolvement at each node, which depends on whether the room is disinfected or not. Here, M is a big number. Variable types and sign restrictions are specified by (13).

## 3.4 Numerical experiment

To validate the proposed MIP model and test the maximum of the nodes that can be handled by using Gurobi, a popular optimization solver, we conducted numerical experiments with  $K = \{1, 2, 3\}$ , T = 13, and f = 20. The occupancy and travel distance between nodes were randomly generated. We assumed that travel distances follow the triangular relationship. By increasing the number of rooms, |N|, from 4 to 11, a set of nodes ranging from 20 to 60 were also generated. The node sets and related occupancy were shown in Appendix A (Table A.1 and Table A.2). We implemented the experiment in Python on a PC (INTEL i7-8750H CPU 2.20 GHz with 16 GB RAM). Each scene was run 10 times, followed by the calculation of the average.

When  $K = \{1\}$ ,  $K = \{1, 2\}$  and  $K = \{1, 2, 3\}$ , the average CPU time is shown in Figure 2(a), 1(b) and 1(c), respectively.

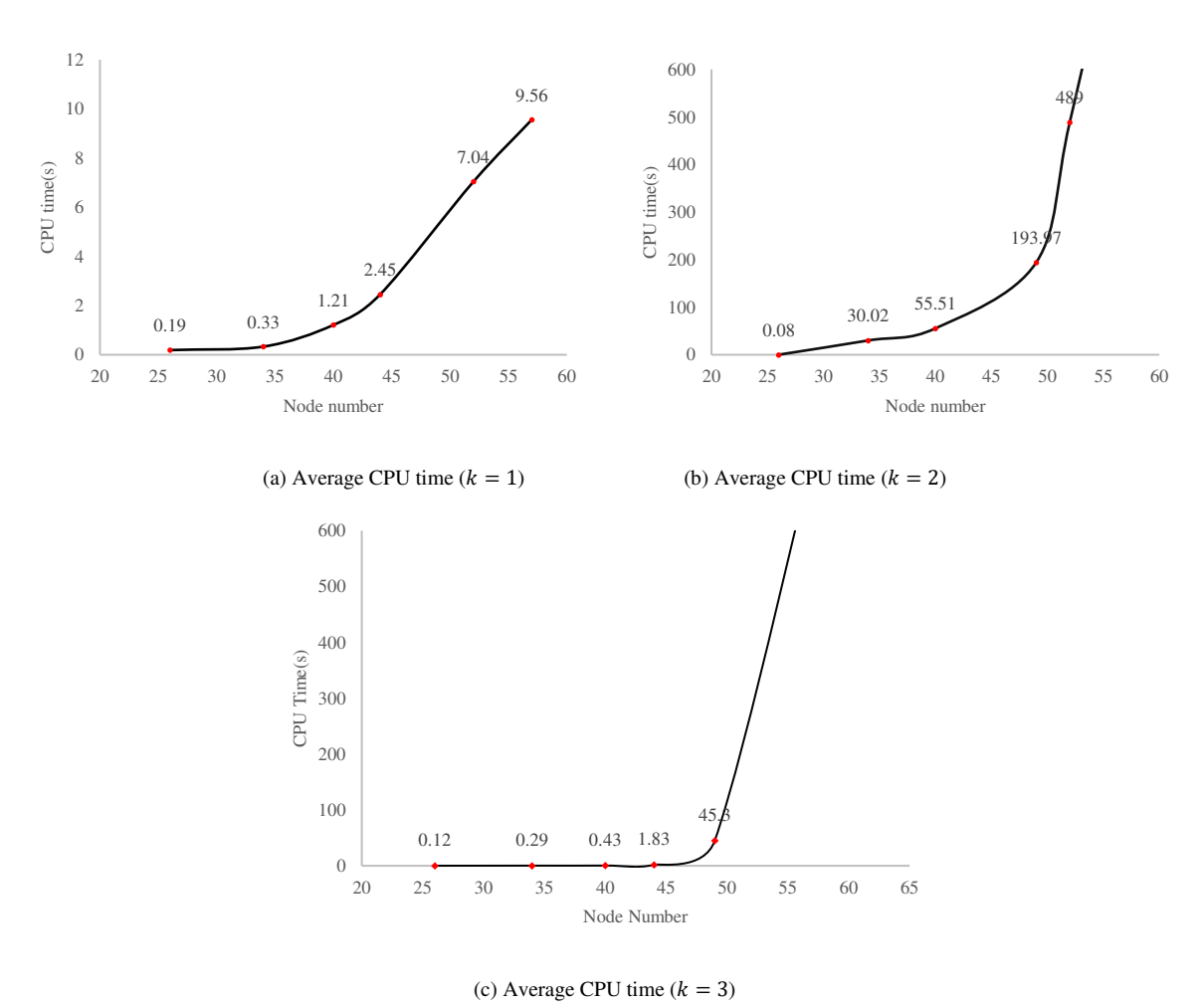


Figure 2. Average CPU time

As shown in Figure 2(a), when  $K = \{1\}$ , Gurobi can deal with 60 nodes within 10 seconds. Figure 2(b) and 2(c) show that in the cases of  $K = \{1, 2\}$  and  $K = \{1, 2, 3\}$ , it took approximately 200 seconds for Gurobi to solve the MIP model when the number of nodes was less than 50, after which the CPU time increased exponentially. In our real cases of a teaching building on our campus, the number of nodes was less than 50, which means Gurobi can solve the case study successfully. However, if we consider a scheduling problem with multiple buildings, the number of nodes will well exceed 200 and Gurobi cannot handle it.

In order to demonstrate the superiority of MIP results over other algorithms, High Risk First (HRF) and Nearby Search (NS) were designed considering a single disinfection robot. The results and CPU time of MIP, HRF and NS are shown in the Table. The pseudocodes of HRF and NS were shown below.

```
Algorithm High Risk First (HRF)
      Initialize \Phi as a list for the final schedule, \Upsilon as a list for the travel time between nodes
2:
      including depot. Let T be the number of time window, and P be the number of rooms.
3:
      Start from the depot (node 0).
4:
      for t in range 0 to T-1:
5:
         for i in range 0 to P-1:
6:
             Initialize tmp as 0, a list R to store risks for each node, a list U to store the index of
7:
             the node corresponding to the risk in R
8:
            Calculate the risk of each node in time window t and add them to R
9:
             Sort R in descending order, and update U accordingly
10:
             Calculate the travel time between nodes in time window t, add them into \Upsilon
11:
            if t = 0
12:
                  if travel time W_{0u} \le \text{time window } t \text{ duration for the first node } u \text{ in } U
13:
                      tmp = tmp + W_{0u}
14:
                      Add the node u to the list \Phi
15:
                   for each subsequent node v in U:
                      if travel time W_{uv} \le \text{time window } t \text{ duration (where } u = \Phi[-1])
16:
17:
                         tmp = tmp + W_{uv}
18:
                         Add the node v to the list \Phi
19:
             else
20:
                   for each node v in U:
21:
                      if travel time W_{uv} \le \text{time window } t \text{ duration (where } u = \Phi[-1])
22:
                         tmp = tmp + W_{uv}
23:
                         Add the node v to the list \Phi
24:
      Output \Phi as the disinfection schedule. Calculate and output the total risk.
25:
```

```
Algorithm Nearby Search (NS)
1:
      Initialize \Phi as a list for the final schedule, \Upsilon as a list for the travel time between nodes
2:
      including depot. Let T be the number of time window, and P be the number of rooms.
3:
      Start from the depot (node 0).
4:
      for t in range 0 to T-1:
5:
         for i in range 0 to P-1:
6:
             Initialize tmp as 0, a list D to store the distance between nodes, a list U to store the
7:
             index of the node corresponding to the distance in D
             Calculate the distance of nodes in time window t and add them to D
8:
9:
             Sort D in ascending order, and update U accordingly
10:
             Calculate the travel time between nodes in time window t, add them into \Upsilon
            if t = 0
11:
12:
                  if travel time W_{0u} \le \text{time window } t \text{ duration for the first node } u \text{ in } U
13:
                      tmp = tmp + W_{0u}
14:
                      Add the node u to the list \Phi
15:
                   for each subsequent node v in U:
16:
                      if travel time W_{uv} \le \text{time window } t \text{ duration (where } u = \Phi[-1])
17:
                      tmp = tmp + W_{uv}
18:
                      Add the node v to the list \Phi
19:
             else
20:
                   for each node v in U:
                      if travel time W_{uv} \le \text{time window } t \text{ duration (where } = \Phi[-1])
21:
22:
                      tmp = tmp + W_{uv}
23:
                      Add the node v to the list \Phi
24:
      Output \Phi as the disinfection schedule. Calculate and output the total risk.
25:
      End
```

Table. Results and CPU time of MIP, HRF, and NS

Number of	N	1IP	F	IRF		NS
nodes	Result	CPU time	Result	CPU time	Result	CPU time
20	4.268	0.11	4.268	0.07	8.143	0.09
40	8.534	0.39	9.534	0.11	16.62	0.13
60	19.459	7.59	22.119	2.11	36.43	3.24
80	25.831	8.66	29.372	5.16	57.33	6.44
100	30.164	9.54	36.842	10.2	67.16	8.15

As depicted in Table, the CPU time of NS is shortest under these five scenarios, followed by HRF and MIP. If the room was cleaned using the NS, the infection risk will be reduced but still greater at most 45% and 55% than HRF and MIP, respectively. We can see from Table that when the number of nodes is 20, the results of MIP and HRF are the same. However, the HRF greedy algorithm cannot guarantee the global optimal solution to larger scale problems. When the number of nodes is moderate (below 100), MIP can get the best results which can reduce the infection risk by up to 18% compared with HRF.

### 4. Case (A single building model with Gurobi solution)

### 4.1 Base solution with digital presentation

In this study, a building in the University of Tennessee, Knoxville, named Mossman Hall, was used as

a case to demonstrate the room infection risk calculation and scheduling optimization. The case considers a typical week of the 2022 Spring semester. There are seven classrooms in the building. As stated in Section 3.1, the required information to assess the room infection risks includes room characteristics, occupant characteristics, disinfection information, and pathogen-specific parameters. The accessible surfaces are considered as the room characteristic and were computed as the average value of the seven classrooms. The method of the retrieval of the accessible surface via BIM is described in our previous paper. For each room, the occupant characteristics were retrieved from the classroom schedule, including the number of classes and breaks for a day, the duration of each class, and the number of students enrolled in each class. For disinfection activities, it is assumed that the disinfection robot can disinfect the classroom during class breaks, and disinfection strategies could eliminate all the pathogens in the room.

To assess the infection risks of each classroom  $i \in N$ , a revised fomite-based pathogen transmission model was developed in this study. For the original environmental infection transmission system (EITS) model, it is assumed that the environment is an isolated system with a constant population size. However, this assumption proves inadequate when applied to classroom settings, where individuals enter and exit frequently, and the population is far from constant. Consequently, a revised model is developed to accurately estimate infection risks in each classroom, accounting for varying schedules during the academic year, incorporating disinfection activities between classes.

In particular, the model addresses the dynamic nature of classroom populations over time. Notably, during class breaks, when no occupants are using the classroom, there is no pathogen transmission. Moreover, disinfection activities may take place during breaks. This leads to three significant differences between the improved fomite-based pathogen transmission model and its predecessor.

First, the assumption of an isolated environment for the entire planning horizon was relaxed. Instead, the revised model considers each class as an isolated space with a constant population size. The initial number of pathogens on surfaces in each classroom can be inherited from the remaining pathogens surviving on surfaces from the previous class to the current class. The second difference is the consideration of breaks in the school scenario. During these breaks, there is no pathogen transmission. Following each break, a new group of occupants enters the classroom. The pool of pathogens capable of infecting occupants comprises those inherited from previous classes after the latest disinfection and the pathogens generated in the current class. The third consideration pertains to disinfection activities. Unlike the previous model, which set the disinfection rate at a constant frequency (e.g., time per day), our situation requires a more nuanced approach. Disinfection cannot occur when the classroom is occupied by students, limiting opportunities within breaks. Moreover, we aim to optimize the disinfection schedule, introducing variability in frequency. Additionally, we factor in the impact of disinfection on consecutive classes following the disinfection event.

In our study, due to the consideration of time-varying room occupancy in a day, we assume that 1) the environment of each class is an isolated system, and the influence from previous classes is simplified as the remaining pathogens; 2) there is one infector for each class. In our model, the infection risk is defined as the number of susceptible individuals being infected in each class and can be computed using equation (1-3) in Section 3.2, and equation (13-17).

$$P_{pick,v} = \frac{M_v \rho_{FH}}{M_v \rho_{FH} + \mu_F} \tag{13}$$

$$K_{F,v} = T_v a_F P_{inoc} P_{vickuv,v} P'(0)$$
(14)

$$K_{Hv} = T_v a_H P_{inoculation} P_{deposit} P_{pickup,v} P'(0)$$
(15)

$$K_{R,v} = \sum_{j \in V_i^v} (T_j (a_F + a_H P_{deposit}) - \mu_F T_{b,j} - T_j N_j \rho_{FH}) P_{inoculation} P_{pickup,iv} P'(0)$$
(16)

$$K_{v} = K_{F,v} + K_{H,v} + K_{R,v} \tag{17}$$

The detailed flowchart for room infection risk calculation is illustrated in Figure 3. To compute the number of remaining pathogens for each classroom, the process starts with checking if the current class is the first class of the day. If it is the first class, the remaining pathogen equals 0; if it is not the first class, it should be checked if the disinfection action occurs in the break just before this class. If the classroom is disinfected, the remaining pathogen is 0; if not, the number of remaining pathogens

generated before this class is computed using equation (16), and the infection risk of this classroom can be computed using equation (17). The calculation process loops over all possible disinfection actions (e.g., disinfect or not) in each break, and computes all possible infection risks for each class in each classroom.

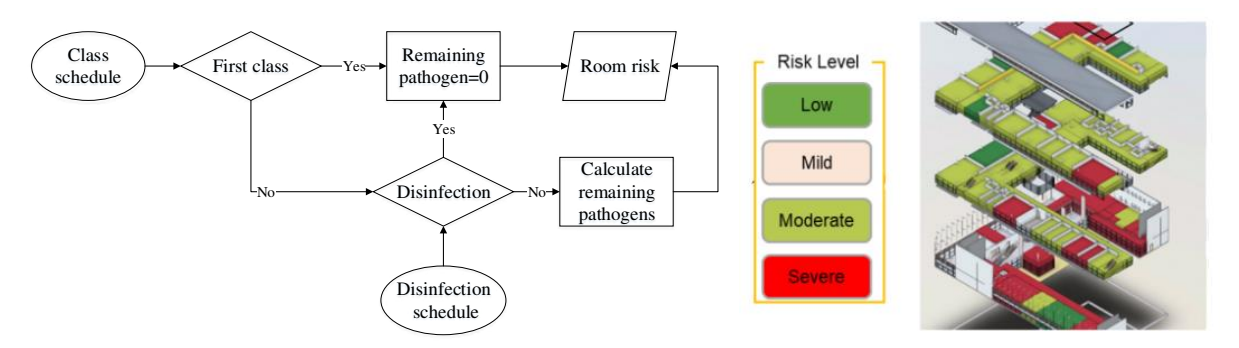


Figure 3. The flowchart of room infection risk calculation

Figure 4. Pathogen transmission visualization

Using the revised model, the relative exposure risk can thereby be derived for each building compartment (room), as demonstrated in Figure 4. This information is instrumental in guiding building management. However, to achieve precise control and effectively guide the scheduling of cleaning robots, it is essential to integrate it with our optimization model.

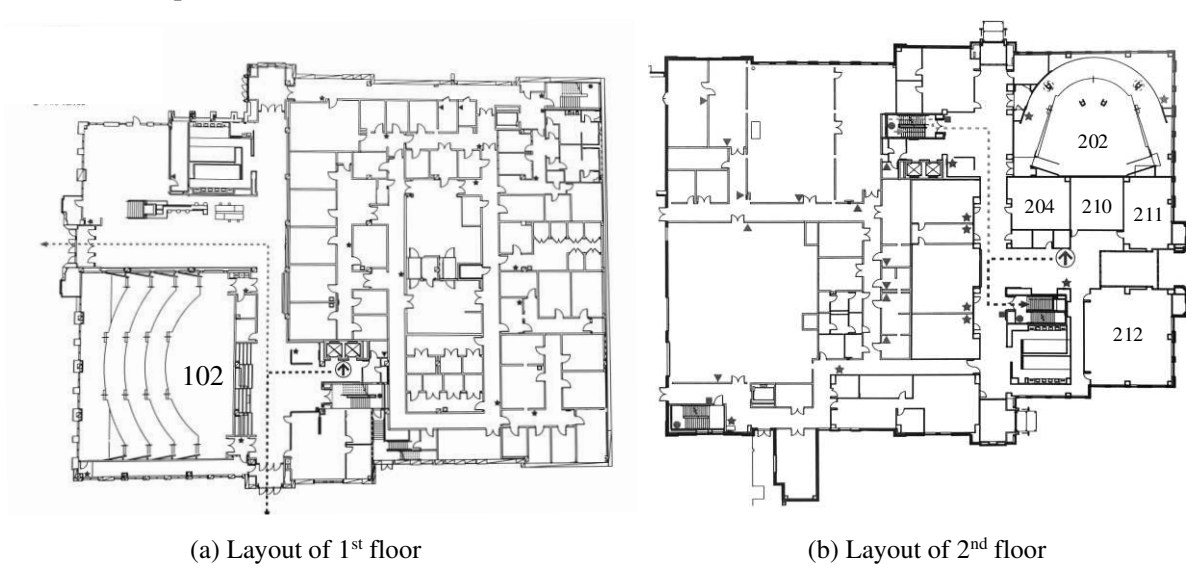
## 4.2 A single building model with Gurobi solution

In real case, the weekly class schedule of an academic building is shown in Figure 5, and the lists of node u = (i, t) from Monday to Friday are shown in the Appendix A (Tables A.4-A.6). The occupancy of each room in the different time windows are presented in Appendix A (Tables A.7-A.9). Figure 6 shows the layout of each floor. Assuming there is no obstacle avoidance for robots, their traveling distance between rooms will take the shortest path. The risk sets are calculated by the equations from Section 4.1 based on the time window and occupancy in the Appendix.



Figure 5. Weekly class schedule

The speed of robot and the cleaning time of each room are assumed to be 2 m/min and 20 min, respectively. To obtain the optimal results, the experiments are implemented in Python on a PC (INTEL i7-8750H CPU 2.20 GHz with 16 GB RAM). Taking Monday, Wednesday and Friday for example, the average CPU time for  $K = \{1\}$ ,  $K = \{1,2\}$  and  $K = \{1,2,3\}$  to solve the MIP model by GUROBI solver is 0.01s. The optimal solutions are shown below:



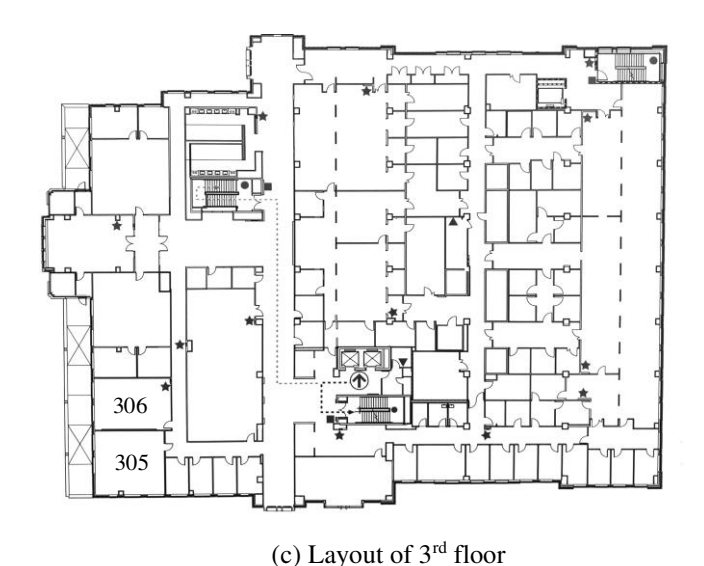


Figure 6. Classroom layouts

### Monday:

- (1) The optimal value of  $K = \{1\}$  is 0.2766 and the optimal scheduling is as follows:  $0 \text{ (depot)} \rightarrow 1(1,2) \rightarrow 12 (2,4) \rightarrow 24 (3,6) \rightarrow 14 (2,8) \rightarrow 8(1,10) \rightarrow 9(1,12) \rightarrow 50 \text{ (depot)}$
- (2) The optimal value of  $K = \{1,2\}$  is 0.0036, and the optimal scheduling is as follows Robot #1: 0 (depot)  $\rightarrow$  12 (2,4)  $\rightarrow$  13 (2,6)  $\rightarrow$  14 (2,8)  $\rightarrow$  35 (4,10)  $\rightarrow$  28 (3,12)  $\rightarrow$  50(depot) Robot #2: 0 (depot)  $\rightarrow$  1(1,2)  $\rightarrow$  24 (3,6)  $\rightarrow$  25 (3,8)  $\rightarrow$  8(1,10)  $\rightarrow$  9(1,12)  $\rightarrow$  50(depot)
- (3) The optimal value of  $K = \{1,2,3\}$  is 0, and the optimal scheduling is as follows Robot #1: 0 (depot)  $\rightarrow$ 12 (2,4)  $\rightarrow$ 24 (3,6)  $\rightarrow$ 25 (3,8)  $\rightarrow$ 8(1,10)  $\rightarrow$  9(1,12)  $\rightarrow$ 50(depot) Robot #2: 0 (depot)  $\rightarrow$ 1(1,2)  $\rightarrow$ 28 (3,12)  $\rightarrow$ 50(depot) Robot #3: 0 (depot)  $\rightarrow$ 13 (2,6)  $\rightarrow$ 14(2,8)  $\rightarrow$ 49(5,12)  $\rightarrow$ 50(depot)

#### Wednesday:

- (1) The optimal value of  $K = \{1\}$  is 0.2126 and the optimal scheduling is as follows  $0 \text{ (depot)} \rightarrow 1(1,2) \rightarrow 13 (2,4) \rightarrow 14 (2,6) \rightarrow 26 (3,8) \rightarrow 8(1,10) \rightarrow 9(1,12) \rightarrow 30 \text{ (depot)}$
- (2) The optimal value of  $K = \{1,2\}$  is 0, and the optimal scheduling is as follows Robot #1: 0 (depot)  $\to$  14 (2,6)  $\to$  29 (3,12)  $\to$ 30(depot) Robot #2: 0 (depot)  $\to$ 1(1,2)  $\to$ 13 (2,4)  $\to$ 25 (3,6)  $\to$ 26 (3,8)  $\to$  8(1,10)  $\to$ 9(1,12)  $\to$ 30(depot)

## Friday:

- (1) The optimal value of  $K = \{1\}$  is 0.1206 and the optimal scheduling is as follows  $0 \text{ (depot)} \rightarrow 1(1,2) \rightarrow 13 (2,4) \rightarrow 14 (2,6) \rightarrow 26 (3,8) \rightarrow 8(1,10) \rightarrow 9(1,12) \rightarrow 31 \text{ (depot)}$
- (2) The optimal value of  $K = \{1,2\}$  is 0, and the optimal scheduling is as follows Robot #1: 0 (depot)  $\to$ 13 (2,4)  $\to$ 14 (2,6)  $\to$ 8(1,10)  $\to$  31(depot) Robot #2: 0 (depot)  $\to$ 1(1,2)  $\to$ 25 (3,6)  $\to$ 26 (3,8)  $\to$ 9(1,12)  $\to$ 31(depot)

In addition, several experiments were conducted to compare the solution of our model with other

cleaning policies such as cleaning based on HRF, NS, random cleaning (shown below) and not cleaning.

```
Algorithm Random Cleaning
        Initialize \Phi as a list for the schedule, P be the number of rooms, T be the number of time windows
1:
2:
        Q is a P \times T node matrix, \Lambda is a set of nodes related to the objective function
3:
4:
           Initialize \Phi_k as the subset of \Phi, tmp<sub>k</sub> = []
5:
           for t in range 0 to T-1:
6:
              for i in range 0 to P-1:
7:
                  for each \lambda \in \Lambda:
8:
                     if (\lambda is not in \Phi):
9:
                          Initialize \rho be the lens of list \Phi_k
                          if (\Phi_k \neq \emptyset) and t == \operatorname{tmp}_k[\rho - 1] and travel time \leq time window t duration):
10:
11:
                              \Phi_k. append (Q_{i,t})
12:
                               tmp_k. append(t)
13:
                          else:
14:
                              \Phi_k append (Q_{i,t})
15:
                              tmp_k. append(t)
16:
        Output \Phi as the disinfection schedule. Calculate and output the total risk.
17:
        End
```

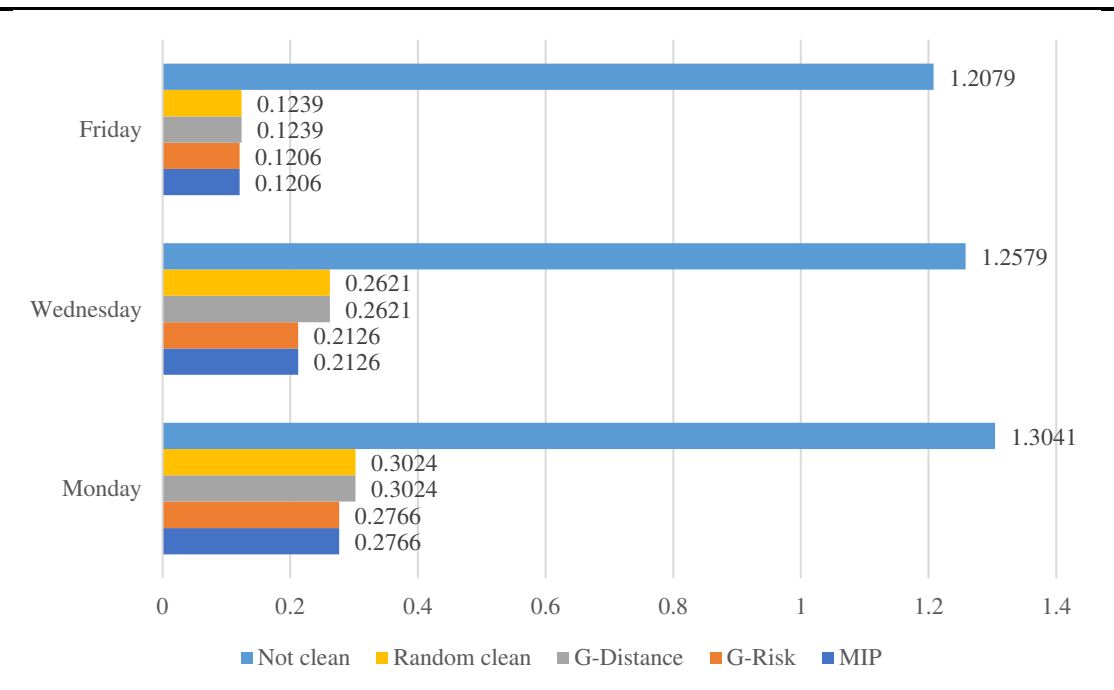


Figure 7. Comparation of five different results: not clean, random clean, HRF, NS, and MIP when k = 1

Figure 7 shows the infection risks of 5 different cleaning policies. As we can see, if the rooms were not cleaned, the infection risk is as high as 1.304. If the room was cleaned randomly or using NS algorithm, the infection risk will be reduced but still greater than optimal solution. Compared with random clean and NS, MIP solutions can reduce the infection risk by up to 18%. Compared with the not cleaning solution, MIP can also reduce the infection risk by up to 90%. HRF can get the same optimal result as MIP in this case. However, the greed algorithm cannot guarantee the global optimal solution to larger scale problems. Based on the comparisons, the MIP model can reduce the infection risks effectively.

### 4.3 Sensitivity analysis

### 4.3.1 Sensitivity analysis for infection risk assessment

In this subsection, we have considered various pathogens in our analysis that may pose future public health risks, such as influenza and rhinovirus. The input parameters to the infection risk calculation regarding influenza and rhinovirus are shown in Appendix A (Table A.10 and A.11, respectively).

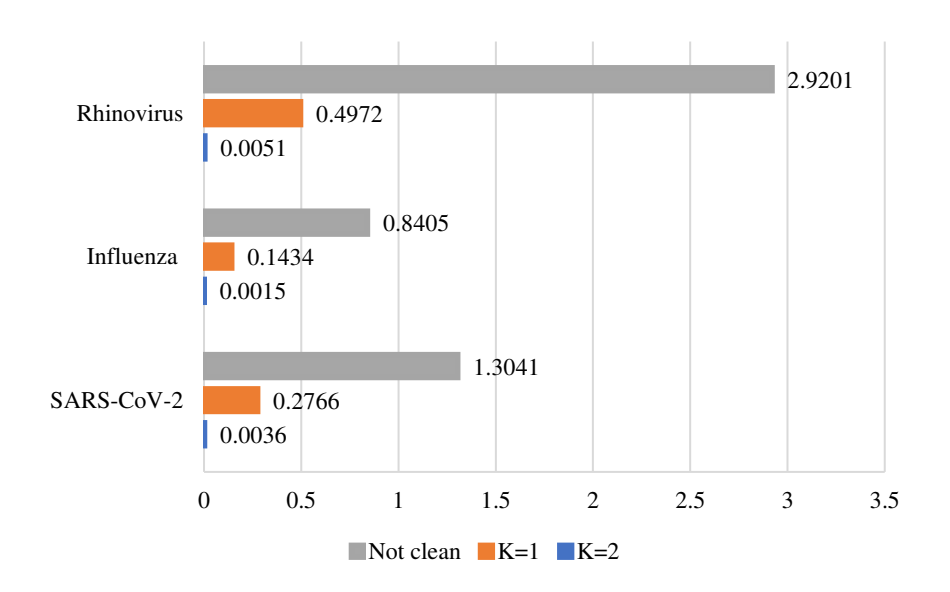


Figure 8. Comparation of three different results: SARS-CoV-2, Influenza, Rhinovirus on Monday

Figure 8 illustrates that among the three scenarios presented, the risk posed by rhinovirus is the most pronounced, followed by SARS-CoV-2 and influenza. Rhinovirus has a higher risk due to its highly efficient transmission, longer periods of shedding, and persistence on hands and surfaces. In comparison, the risks associated with influenza are relatively low risk due to its higher surface die-off rates[18]. If we implement a single disinfection robot (k = 1), the risks of all three pathogens can be reduced by a range of 78% to 83%. The reduction in risk can be enhanced to as much as 99% by increasing the number of robots.

The significant impact of this intervention is not limited to COVID-19 only, but it can also be applied to potential future outbreaks of other infectious diseases. Our findings provide more comprehensive and forward-looking strategies to better manage and contain potential outbreaks.

### 4.3.2 Sensitivity analysis for optimization

In this subsection, different speed and cleaning time of robot are considered, and how these factors affect the optimal value is analyzed. Increasing the robot speed within a reasonable range can reduce the wasted time between rooms. Additionally, when the necessary cleaning time can be shortened, it is

more likely for robots to travel to all the rooms that need to be cleaned. However, it usually occurs when the disinfection method can be decided by robots after receiving the virus information from the sensors. Herein, the decision-making of the disinfection method is not the focus of our research, and the cleaning time of each room is assumed to be flexible.

An algorithm is proposed to help to find the optimal speed within a reasonable range.

```
Algorithm Optimal Speed
        Let C be the maximum value robots can reach
1:
2:
        Set \varphi = 1, initialize \Omega_{pre} to a large value, set tolerance level =0.01
3:
        While \varphi < C
             calculate the value of objective function \Omega_{\omega}
4:
5:
             if |\Omega_{\varphi} - \Omega_{pre}| < \text{tolerance level}
6:
                 break
             if (\Omega_{\omega} = 0)
7:
8:
                  Set optimal speed \Psi_{optimal} = \varphi and \Omega_{optimal} = 0
9:
10:
             else calculate the value of objective function \Omega_{\varphi+1}
11:
                  if (\Omega_{\varphi+1} < \Omega_{\varphi})
                          \Psi_{optimal} = \varphi + 1 and \Omega_{optimal} = \Omega_{\varphi+1} then \varphi = \varphi + 1
12:
13:
            Set \Omega_{pre} = \Omega_{\varphi}
14:
        Output \Psi_{optimal} and \Omega_{optimal}
15:
        Get the optimal solution for \Psi_{optimal} and \Omega_{optimal}
16:
        End
```

Keeping the cleaning time unchanged, the speed of the robot is changed from the range of 10 to 20 m/min. The relationship between robot speeds and optimal value on Monday, Wednesday and Friday are shown in Figures 9,10, and 11, respectively.

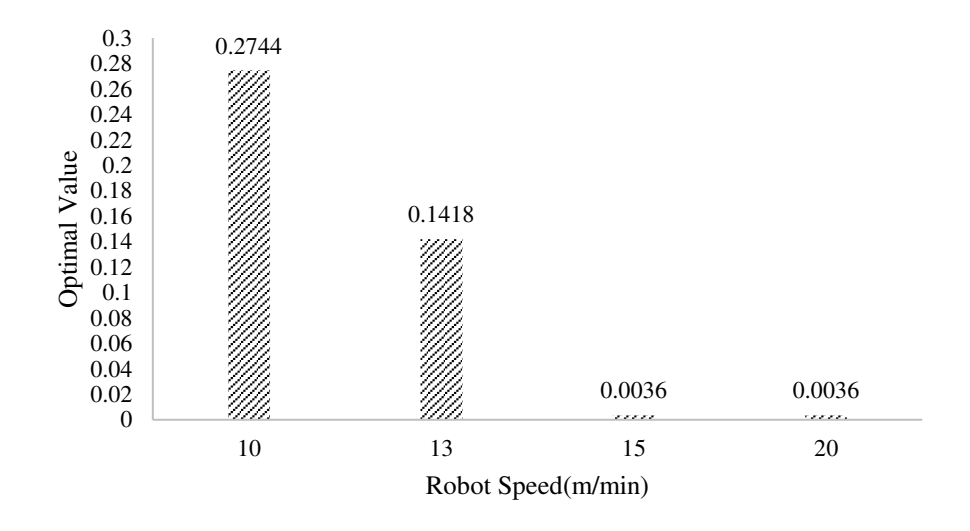


Figure 9. Sensitivity analysis of Monday

The optimal solutions for Monday based on the different robot speeds are shown below. It changed since the optimal value has been changed, which is obtained from the previous algorithm.

(1) Robot speed: 10-12 m/min

$$0 \text{ (depot)} \rightarrow 1(1,2) \rightarrow 12 (2,4) \rightarrow 24 (3,6) \rightarrow 14 (2,8) \rightarrow 35 (4,10) \rightarrow 8(1,10) \rightarrow 9(1,12) \rightarrow 50 \text{ (depot)}$$

(2) Robot speed: 13-14 m/min

$$0 (depot) \rightarrow 1(1,2) \rightarrow 12(2,4) \rightarrow 24(3,6) \rightarrow 13(2,6) \rightarrow 25(3,8) \rightarrow 14(2,8) \rightarrow 8(1,10) \rightarrow 35(4,10) \rightarrow 9(1,12) \rightarrow 50(depot)$$

(3) Robot speed: 15-20 m/min

$$0 \text{ (depot)} \rightarrow 1(1,2) \rightarrow 12 (2,4) \rightarrow 13(2,6) \rightarrow 24 (3,6) \rightarrow 25(3,8) \rightarrow 14 (2,8) \rightarrow 8(1,10) \rightarrow 35 (4,10) \rightarrow 28(3,12) \rightarrow 9(1,12) \rightarrow 50 \text{(depot)}$$

As can be seen from figure 9, when the speed reaches 20 m/min, the optimal value is not 0, which means that there are some rooms needed to be cleaned. Since the speed of the robot is already very large, we have changed the cleaning time of the robot from 20 min to 9 min. The optimal solution is shown below and the optimal value is 0.

$$0 \text{ (depot)} \rightarrow 1(1,2) \rightarrow 12 \text{ (2,4)} \rightarrow 13(2,6) \rightarrow 24 \text{ (3,6)} \rightarrow 25(3,8) \rightarrow 14 \text{ (2,8)} \rightarrow 8(1,10) \rightarrow 35 \text{ (4,10)} \rightarrow 28(3,12) \rightarrow 49(5,12) \rightarrow 9(1,12) \rightarrow 50 \text{ (depot)}$$

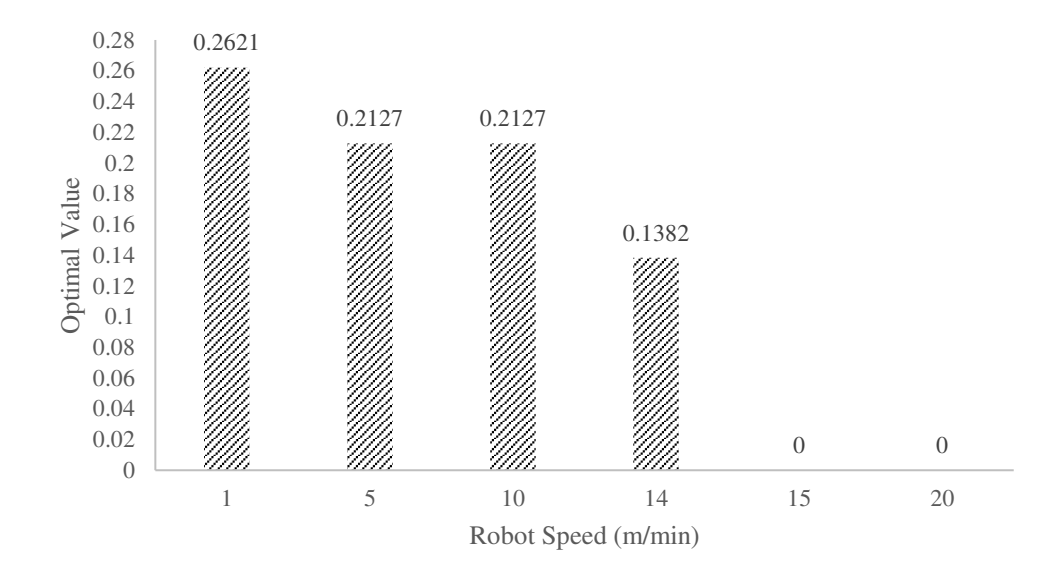


Figure 10. Sensitivity analysis of Wednesday

The optimal solutions for Wednesday based on the different robot speeds are shown below.

(1) Robot speed: 5-13 m/min

$$0 \text{ (depot)} \rightarrow 1(1,2) \rightarrow 13 (2,4) \rightarrow 14 (2,6) \rightarrow 26 (3,8) \rightarrow 8(1,10) \rightarrow 9(1,12) \rightarrow 30 \text{ (depot)}$$

(2) Robot speed: 14 m/min

$$0 \text{ (depot)} \rightarrow 1(1,2) \rightarrow 13 (2,4) \rightarrow 25(3,6) \rightarrow 14 (2,6) \rightarrow 26 (3,8) \rightarrow 8(1,10) \rightarrow 9(1,12) \rightarrow 30 \text{ (depot)}$$

(3) Robot speed: 15-20 m/min

0 (depot)  $\rightarrow$ 1(1,2)  $\rightarrow$  13 (2,4)  $\rightarrow$ 25(3,6)  $\rightarrow$  14 (2,6)  $\rightarrow$ 26 (3,8)  $\rightarrow$ 8(1,10)  $\rightarrow$ 9(1,12)  $\rightarrow$ 29 (3,12)  $\rightarrow$ 30(depot)

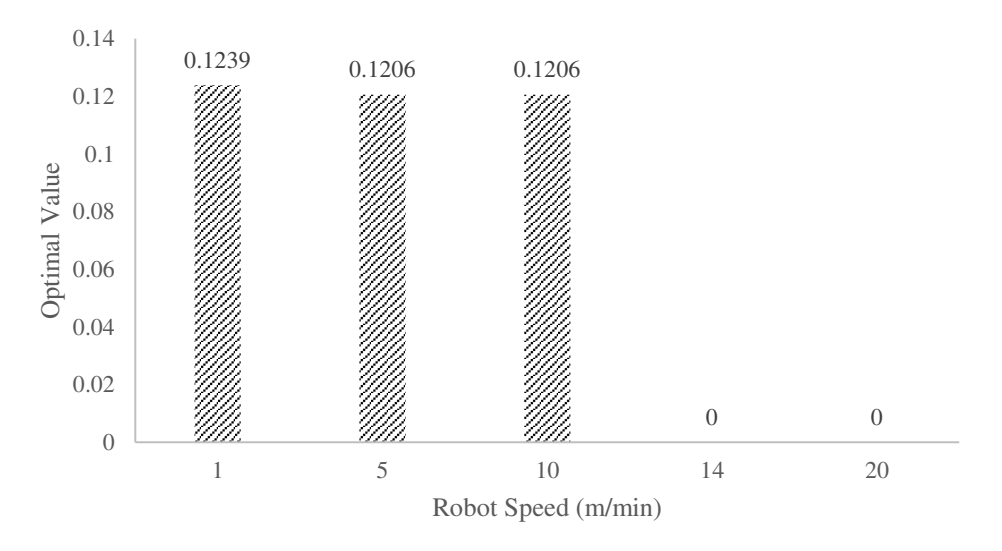


Figure 11. Sensitivity analysis of Friday

The optimal solutions for Friday are shown as follows.

(1) Robot speed: 2-13 m/min  $0 \text{ (depot)} \rightarrow 1(1,2) \rightarrow 13 \text{ (2,4)} \rightarrow 14 \text{ (2,6)} \rightarrow 26 \text{ (3,8)} \rightarrow 8(1,10) \rightarrow 9(1,12) \rightarrow 31 \text{ (depot)}$ 

(2) Robot speed: 14-20 m/min 
$$0 \text{ (depot)} \rightarrow 1(1,2) \rightarrow 13 (2,4) \rightarrow 14 (2,6) \rightarrow 25(3,6) \rightarrow 26 (3,8) \rightarrow 8(1,10) \rightarrow 9(1,12) \rightarrow 31 \text{ (depot)}$$

The schedule for Wednesday is almost the same as that for Friday, so their optimal solutions are very similar. Meanwhile, as can be seen from Figures 10 and 11, keeping the cleaning time of the robot unchanged and increasing its speed can meet all cleaning needs, which is suitable for limited robots and few nodes.

The results intuitively show that when operating on a higher speed, the robots clean the room more efficiently, and we have a lower risk of infection. This is particularly used when we only have limited number of robots.

Using the MIP model, the optimal risk value can be obtained according to different parameters of the disinfection robot. When the infection risk needs to be 0, the minimum number of robots is easy to obtain. Also, we can get the optimal speed by Optimal Speed Algorithm when the number of robots is limited. In this way, we can minimize the infection risk based on cost control of the total robots.

#### 5. Discussion and Conclusion

This study examined the disinfectant robot scheduling problem in classroom buildings. To assess the

infection risks of each classroom, a revised fomite-based pathogen transmission model was developed. To minimize the infection risk, a mathematical model for optimal robot scheduling was proposed. Numerical experiments were randomly generated to test the performance of the mathematical model. The numerical results indicated that problems with rooms below 50 can be solved to their optimality with commercial solvers (e.g., Gurobi). To demonstrate the superiority of MIP results over other algorithms, High Risk First (HRF) and Nearby Search (NS) were designed. The experiments showed that (1) the CPU time of NS was shortest under these five scenarios, followed by HRF and MIP. (2) the results of total risk of MIP were smallest, followed by HRF and NS. An academic building was used as a case study to demonstrate the room infection risk calculation and disinfection robot scheduling optimization. Compared with random clean and NS, MIP solutions can reduce the infection risk by up to 18%. Compared with the not cleaning solution, MIP reduced the infection risk by up to 90%. HRF obtained the same optimal result as MIP in this case. However, the greed algorithm cannot guarantee the global optimal solution to larger scale problems. The sensitivity analyses included various pathogens that may pose future public health risks, such as influenza and rhinovirus. The significant impact of our strategies indicates potential future applications for other infectious disease outbreaks. The Optimal Speed algorithm was designed to help decision makers find the optimal speed within a reasonable range. Through a case study, we obtained the following two insights. (1) the optimized scheduling obtained by MIP model can reduce the infection risks effectively. (2) When facing fewer number of disinfection robots, we can increase robot speed within a reasonable range to reduce the infection risk.

In our study, we considered the average speed of robots and the shortest path between two locations, which ignored the obstacle avoidance time of robots. In addition, we assumed the cleaning time is fixed. However, cleaning time varied from room to room based on the different pathogen densities and cleaning methods. Therefore, in future studies, we will consider the stochastic travel time of robots and cleaning time for rooms in the classroom building. In addition, the scheduling problem in this study was based on a certain scenario, because the time windows of classrooms were fixed. In some other scenarios, such as the consultation room and operation room in the hospital, their time windows were uncertain. So, we will also consider the stochastic time windows under uncertain scenarios in further study.

This study linked fomite-based pathogen prediction with disinfection robot scheduling to reduce the infection risks at the building and room level, filling a notable gap in the current literature where such a comprehensive approach is seldom explored. It had a great potential to reduce the exposure risks of building occupants to infectious diseases, eliminating key hotspots of community transmission. The proposed framework could be scalable and adaptable to facilities with different functions, configurations, and sizes. Translating the research outcomes into practice will generate significant and timely broader impacts.

# Acknowledgements

This research was supported by the U.S. National Science Foundation (CPS: Medium: Bio-socially Adaptive Control of Robotics-Augmented Building-Human Systems for Infection Prevention by Cybernation of Pathogen Transmission), grant number 2038967.

#### Reference

- [1] C. Karakosta, Z. Mylona, J. Karásek, A. Papapostolou, E. Geiseler, Tackling covid-19 crisis through energy efficiency investments: Decision support tools for economic recovery, Energy Strategy Reviews 38 (2021) 100764. https://doi.org/10.1016/j.esr.2021.100764.
- [2] N. Shrestha, M.Y. Shad, O. Ulvi, M.H. Khan, A. Karamehic-Muratovic, U.-S.D.T. Nguyen, M. Baghbanzadeh, R. Wardrup, N. Aghamohammadi, D. Cervantes, Kh.M. Nahiduzzaman, R.A. Zaki, U. Haque, The impact of COVID-19 on globalization, One Health 11 (2020) 100180. https://doi.org/10.1016/j.onehlt.2020.100180.
- [3] R. Liu, Disparities in Disruptions to Postsecondary Education Plans During the COVID-19 Pandemic, AERA Open 7 (2021) 23328584211045400. https://doi.org/10.1177/23328584211045400.
- [4] J.A. Gilbert, B. Stephens, Microbiology of the built environment, Nat Rev Microbiol 16 (2018) 661–670. https://doi.org/10.1038/s41579-018-0065-5.
- [5] S. Tang, Y. Mao, R.M. Jones, Q. Tan, J.S. Ji, N. Li, J. Shen, Y. Lv, L. Pan, P. Ding, X. Wang, Y. Wang, C.R. MacIntyre, X. Shi, Aerosol transmission of SARS-CoV-2? Evidence, prevention and control, Environment International 144 (2020) 106039. https://doi.org/10.1016/j.envint.2020.106039.
- [6] S. Rayegan, C. Shu, J. Berquist, J. Jeon, L. (Grace) Zhou, L. (Leon) Wang, H. Mbareche, P. Tardif, H. Ge, A review on indoor airborne transmission of COVID-19– modelling and mitigation approaches, Journal of Building Engineering 64 (2023) 105599. https://doi.org/10.1016/j.jobe.2022.105599.
- [7] K. Ruan, Z. Wu, Q. Xu, Smart Cleaner: A New Autonomous Indoor Disinfection Robot for Combating the COVID-19 Pandemic, Robotics 10 (2021) 87. https://doi.org/10.3390/robotics10030087.
- [8] S. SanJuan-Reyes, L.M. Gómez-Oliván, H. Islas-Flores, COVID-19 in the environment, Chemosphere 263 (2021) 127973. https://doi.org/10.1016/j.chemosphere.2020.127973.
- [9] G.-Z. Yang, B. J. Nelson, R.R. Murphy, H. Choset, H. Christensen, S. H. Collins, P. Dario, K. Goldberg, K. Ikuta, N. Jacobstein, D. Kragic, R.H. Taylor, M. McNutt, Combating COVID-19—The role of robotics in managing public health and infectious diseases, Science Robotics 5 (2020) eabb5589. https://doi.org/10.1126/scirobotics.abb5589.
- [10] H. Yang, M.V. Balakuntala, A.E. Moser, J.J. Quiñones, A. Doosttalab, A. Esquivel-Puentes, T. Purwar, L. Castillo, N. Mahmoudian, R.M. Voyles, Enhancing Safety of Students with Mobile Air Filtration during School Reopening from COVID-19, in: 2021 IEEE International Conference on Robotics and Automation (ICRA), 2021: pp. 10757–10763. https://doi.org/10.1109/ICRA48506.2021.9561857.
- [11] N. Castaño, S.C. Cordts, M. Kurosu Jalil, K.S. Zhang, S. Koppaka, A.D. Bick, R. Paul, S.K.Y. Tang, Fomite Transmission, Physicochemical Origin of Virus–Surface Interactions, and Disinfection Strategies for Enveloped Viruses with Applications to SARS-CoV-2, ACS Omega 6 (2021) 6509–6527. https://doi.org/10.1021/acsomega.0c06335.
- [12] B.F. Leo, C.Y. Lin, K. Markandan, L.H. Saw, M.S. Mohd Nadzir, K. Govindaraju, I.I. Shariffuddin, R. Sankara, Y.W. Tiong, H. Pakalapati, M. Khalid, An overview of SARS-CoV-2 transmission and engineering strategies to mitigate risk, Journal of Building Engineering 73 (2023) 106737. https://doi.org/10.1016/j.jobe.2023.106737.
- [13] T.-W. Tsang, K.-W. Mui, L.-T. Wong, Computational Fluid Dynamics (CFD) studies on airborne transmission in hospitals: A review on the research approaches and the challenges, Journal of Building Engineering 63 (2023) 105533. https://doi.org/10.1016/j.jobe.2022.105533.
- [14] S. Li, Y. Xu, J. Cai, D. Hu, Q. He, Integrated environment-occupant-pathogen information modeling to assess and communicate room-level outbreak risks of infectious diseases, Building and Environment 187 (2021) 107394-. https://doi.org/10.1016/j.buildenv.2020.107394.
- [15] S. Riddell, S. Goldie, A. Hill, D. Eagles, T.W. Drew, The effect of temperature on persistence of SARS-CoV-2 on common surfaces, Virology Journal 17 (2020) 145–145. https://doi.org/10.1186/s12985-020-01418-7.
- [16] F.-C. Jiang, X.-L. Jiang, Z.-G. Wang, Z.-H. Meng, S.-F. Shao, B.D. Anderson, M.-J. Ma, Detection of Severe Acute Respiratory Syndrome Coronavirus 2 RNA on Surfaces in Quarantine Rooms, Emerging Infectious Diseases 26 (2020) 2162–2164. https://doi.org/10.3201/eid2609.201435.
- [17] A.P. Harvey, E.R. Fuhrmeister, M.E. Cantrell, A.K. Pitol, J.M. Swarthout, J.E. Powers, M.L. Nadimpalli, T.R. Julian, A.J. Pickering, Longitudinal Monitoring of SARS-CoV-2 RNA on High-Touch Surfaces in a Community Setting, Environmental Science & Technology Letters 8 (2021) 168–175. https://doi.org/10.1021/acs.estlett.0c00875.
- [18] A.N.M. Kraay, M.A.L. Hayashi, N. Hernandez-Ceron, I.H. Spicknall, M.C. Eisenberg, R. Meza, J.N.S. Eisenberg, Fomite-mediated transmission as a sufficient pathway: a comparative analysis across three viral pathogens, BMC Infectious Diseases 18 (2018) 540–540. https://doi.org/10.1186/s12879-018-3425-x.
- [19] M. Diab-El Schahawi, W. Zingg, G. Vos, H. Humphreys, L. Lopez-Cerero, A. Fueszl, J.R. Zahar, E. Presterl, Ultraviolet disinfection robots to improve hospital cleaning: Real promise or just a gimmick?, Antimicrobial Resistance & Infection Control 10 (2021) 33–33. https://doi.org/10.1186/s13756-020-00878-4.

- [20] S.W. Kembel, E. Jones, J. Kline, D. Northcutt, J. Stenson, A.M. Womack, B.J. Bohannan, G.Z. Brown, J.L. Green, Architectural design influences the diversity and structure of the built environment microbiome, The ISME Journal 6 (2012) 1469–1479. https://doi.org/10.1038/ismej.2011.211.
- [21] R.I. Adams, M. Miletto, J.W. Taylor, T.D. Bruns, The diversity and distribution of fungi on residential surfaces, PloS One 8 (2013) e78866-. https://doi.org/10.1371/journal.pone.0078866.
- [22] S.W. Kembel, J.F. Meadow, T.K. O'Connor, G. Mhuireach, D. Northcutt, J. Kline, M. Moriyama, G.Z. Brown, B.J.M. Bohannan, J.L. Green, Architectural design drives the biogeography of indoor bacterial communities, PloS One 9 (2014) e87093-. https://doi.org/10.1371/journal.pone.0087093.
- [23] H. Yang, M.V. Balakuntala, J.J. Quiñones, U. Kaur, A.E. Moser, A. Doosttalab, A. Esquivel-Puentes, T. Purwar, L. Castillo, X. Ma, L.T. Zhang, R.M. Voyles, Occupant-centric robotic air filtration and planning for classrooms for Safer school reopening amid respiratory pandemics, Robotics and Autonomous Systems 147 (2022) 103919. https://doi.org/10.1016/j.robot.2021.103919.
- [24] Y. Ma, N. Xi, Y. Xue, S. Wang, Q. Wang, Y. Gu, Development of a UVC-based disinfection robot, Industrial Robot 49 (2022) 913–923. https://doi.org/10.1108/IR-10-2021-0227.
- [25] J. Bačík, P. Tkáč, L. Hric, S. Alexovič, K. Kyslan, R. Olexa, D. Perduková, Phollower—The Universal Autonomous Mobile Robot for Industry and Civil Environments with COVID-19 Germicide Addon Meeting Safety Requirements, Applied Sciences 10 (2020) 7682-. https://doi.org/10.3390/app10217682.
- [26] A. Tuleshov, N. Jamalov, N. Imanbayeva, A. Rakhmatulina, Design and construction of a multifunctional disinfection robot, Eastern-European Journal of Enterprise Technologies 1 (2022) 16–23. https://doi.org/10.15587/1729-4061.2022.252045.
- [27] I. Suwarno, W.A. Oktaviani, Y. Apriani, D.U. Rijalusalam, A. Pandey, Potential Force Algorithm with Kinematic Control as Path Planning for Disinfection Robot, Journal of Robotics and Control (JRC) 3 (2022) 107–114.
- [28] F. Dexter, B. Birchansky, R.H. Epstein, R.W. Loftus, Average and longest expected treatment times for ultraviolet light disinfection of rooms, American Journal of Infection Control 50 (2022) 61–66. https://doi.org/10.1016/j.ajic.2021.08.020.
- [29] A. Mor, M.G. Speranza, Vehicle routing problems over time: a survey, 4OR 18 (2020) 129–149. https://doi.org/10.1007/s10288-020-00433-2.
- [30] P. Vansteenwegen, W. Souffriau, D.V. Oudheusden, The orienteering problem: A survey, European Journal of Operational Research 209 (2011) 1–10. https://doi.org/10.1016/j.ejor.2010.03.045.
- [31] A. Gunawan, H.C. Lau, P. Vansteenwegen, Orienteering Problem: A survey of recent variants, solution approaches and applications, European Journal of Operational Research 255 (2016) 315–332. https://doi.org/10.1016/j.ejor.2016.04.059.
- [32] I.-M. Chao, B.L. Golden, E.A. Wasil, The team orienteering problem, European Journal of Operational Research 88 (1996) 464–474.
- [33] H. Tang, E. Miller-Hooks, A TABU search heuristic for the team orienteering problem, Computers & Operations Research 32 (2005) 1379–1407. https://doi.org/10.1016/j.cor.2003.11.008.
- [34] S. Boussier, D. Feillet, M. Gendreau, An exact algorithm for team orienteering problems, 4OR 5 (2007) 211–230. https://doi.org/10.1007/s10288-006-0009-1.
- [35] P. Vansteenwegen, W. Souffriau, G. Vanden Berghe, D. Van Oudheusden, Iterated local search for the team orienteering problem with time windows, Computers & Operations Research 36 (2009) 3281–3290. https://doi.org/10.1016/j.cor.2009.03.008.
- [36] S.-W. Lin, V.F. Yu, A simulated annealing heuristic for the team orienteering problem with time windows, European Journal of Operational Research 217 (2012) 94–107. https://doi.org/10.1016/j.ejor.2011.08.024.
- [37] W. Souffriau, P. Vansteenwegen, G. Vanden Berghe, D. Van Oudheusden, The Multiconstraint Team Orienteering Problem with Multiple Time Windows, Transportation Science 47 (2013) 53–63. https://doi.org/10.1287/trsc.1110.0377.
- [38] Q. Hu, A. Lim, An iterative three-component heuristic for the team orienteering problem with time windows, European Journal of Operational Research 232 (2014) 276–286. https://doi.org/10.1016/j.ejor.2013.06.011.
- [39] A. Gunawan, H.C. Lau, P. Vansteenwegen, K. Lu, Well-tuned algorithms for the Team Orienteering Problem with Time Windows, The Journal of the Operational Research Society 68 (2017) 861–876. https://doi.org/10.1057/s41274-017-0244-1.
- [40] F.V. Fomin, A. Lingas, Approximation algorithms for time-dependent orienteering, Information Processing Letters 83 (2002) 57–62. https://doi.org/10.1016/S0020-0190(01)00313-1.
- [41] Y. Mei, F.D. Salim, X. Li, Efficient meta-heuristics for the Multi-Objective Time-Dependent Orienteering Problem, European Journal of Operational Research 254 (2016) 443–457. https://doi.org/10.1016/j.ejor.2016.03.053.
- [42] C. Verbeeck, P. Vansteenwegen, E.-H. Aghezzaf, The time-dependent orienteering problem with time windows: a fast ant colony system, Annals of Operations Research 254 (2017) 481–505. https://doi.org/10.1007/s10479-017-2409-3.

- [43] A. Gunawan, K.M. Ng, G. Kendall, J. Lai, An iterated local search algorithm for the team orienteering problem with variable profits, Engineering Optimization 50 (2018) 1148–1163. https://doi.org/10.1080/0305215X.2017.1417398.
- [44] W. Hu, M. Fathi, P.M. Pardalos, A multi-objective evolutionary algorithm based on decomposition and constraint programming for the multi-objective team orienteering problem with time windows, Applied Soft Computing 73 (2018) 383–393. https://doi.org/10.1016/j.asoc.2018.08.026.
- [45] V.F. Yu, P. Jewpanya, S.-W. Lin, A.P. Redi, Team orienteering problem with time windows and time-dependent scores, Computers & Industrial Engineering 127 (2019) 213–224. https://doi.org/10.1016/j.cie.2018.11.044.
- [46] Q. Yu, Y. Adulyasak, L.-M. Rousseau, N. Zhu, S. Ma, Team orienteering with time-varying profit, INFORMS Journal on Computing 34 (2022) 262–280.
- [47] H. Zhang, H. Ge, J. Yang, Y. Tong, Review of Vehicle Routing Problems: Models, Classification and Solving Algorithms, Archives of Computational Methods in Engineering 29 (2021) 195–221. https://doi.org/10.1007/s11831-021-09574-x.
- [48] J. Zhao, J.E. Eisenberg, I.H. Spicknall, S. Li, J.S. Koopman, Model analysis of fomite mediated influenza transmission, PloS One 7 (2012) e51984–e51984. https://doi.org/10.1371/journal.pone.0051984.
- [49] J.S. Sobolik, E.T. Sajewski, L.A. Jaykus, D.K. Cooper, B.A. Lopman, A.N.M. Kraay, P.B. Ryan, J.L. Guest, A. Webb-Girard, J.S. Leon, Decontamination of SARS-CoV-2 from cold-chain food packaging provides no marginal benefit in risk reduction to food workers, Food Control 136 (2022). https://doi.org/10.1016/J.FOODCONT.2022.108845.
- [50] T. Kwon, N.N. Gaudreault, J.A. Richt, T. Vilibic-Cavlek, V. Savic, Environmental Stability of SARS-CoV-2 on Different Types of Surfaces under Indoor and Seasonal Climate Conditions, Pathogens 2021, Vol. 10, Page 227 10 (2021) 227. https://doi.org/10.3390/PATHOGENS10020227.
- [51] M. Nicas, D. Best, A study quantifying the hand-to-face contact rate and its potential application to predicting respiratory tract infection, Journal of Occupational and Environmental Hygiene 5 (2008) 347– 352. https://doi.org/10.1080/15459620802003896.
- [52] G.U. Lopez, C.P. Gerba, A.H. Tamimi, M. Kitajima, S.L. Maxwell, J.B. Rose, Transfer Efficiency of Bacteria and Viruses from Porous and Nonporous Fomites to Fingers under Different Relative Humidity Conditions, Applied and Environmental Microbiology 79 (2013) 5728. https://doi.org/10.1128/AEM.01030-13.
- [53] M. Nicas, R.M. Jones, Relative contributions of four exposure pathways to influenza infection risk, Risk Analysis 29 (2009) 1292–1303. https://doi.org/10.1111/J.1539-6924.2009.01253.X.
- [54] X. Zhang, J. Wang, Deducing the Dose-response Relation for Coronaviruses from COVID-19, SARS and MERS Meta-analysis Results, (2020) 2020.06.26.20140624. https://doi.org/10.1101/2020.06.26.20140624.

Appendix A

Table A.1. Node sets through randomly generated

TW Room	1	2	3	4	5	6	7	8	9	10	11	12	13
1	1	0	2	3	0	0	4	0	5	0	6	0	0
2	0	0	7	0	0	8	9	0	10	0	0	0	0
3	11	12	13	14	15	0	0	0	16	17	0	18	19
4	0	20	21	22	23	24	0	0	0	0	25	0	26
5	0	27	28	29	30	0	31	0	0	32	0	33	34
6	35	0	36	37	0	38	0	0	0	39	40	0	0
7	0	41	0	0	42	0	0	0	0	43	44	0	0
8	0	45	0	0	46	0	0	47	48	0	49	0	0
9	0	0	0	50	51	0	0	0	0	0	52	0	0
10	53	54	55	0	0	56	0	0	57	0	0	0	0
11	58	0	59	60	61	0	0	62	63	64	0	65	0

Table A.2. Occupancy of classroom through randomly generated

									0	, , , ,	J		
TW Room	1	2	3	4	5	6	7	8	9	10	11	12	13
1	0	28	0	0	28	22	0	22	0	21	0	25	22
2	29	27	0	25	25	0	0	29	0	26	29	29	25
3	0	0	0	0	0	22	29	26	0	0	21	0	0
4	28	0	0	0	0	0	21	20	28	25	0	20	0
5	26	0	0	0	0	25	0	24	22	0	29	0	0
6	0	29	0	0	24	0	25	23	29	0	0	27	21
7	22	0	23	26	0	25	24	24	21	0	0	28	27
8	21	0	29	22	0	23	24	0	0	24	0	24	29
9	20	25	24	0	0	23	22	27	20	26	0	22	27
10	0	0	0	25	27	0	27	25	0	26	21	26	24
11	0	26	0	0	0	20	27	0	0	0	22	0	26

Table A.3. Input parameters to the fomite-based transmission model

Parameter	Units	Description	Values	References
	Pathogens/			
α	$(hr \times people)$	Shedding rate	1.99E4	[14]
ρ	/min	Inoculation	0.8	[49]
$\mu_F$	/day	Viral decay rate on F	0.18	[50]
$\mu_H$	/min	Viral decay rate on H	1.195	[51]
		Viral transfer efficiency from F to		
$ au_{FH}$	proportion	Н	0.217	[52]
		Viral transfer efficiency from <i>H</i> to		
$ au_{HF}$	proportion	F	0.025	[53]
$arphi_H$	proportion	Pathogen excreted to <i>H</i>	0.15	[18]
$\pi$	Unitless	Dose-response on mucosa	6.58E-06	[54]
	$1/(days \times$			
$ ho_{FH}$	people)	rate pathogens from $F$ to $H$	$ ho_T  au_{FH} \kappa$	[18]
	$1/(days \times$			
$ ho_{HF}$	people)	rate pathogens from $H$ to $F$	$ ho_T au_{FH}$	[18]
	Pathogens/			
$a_H$	$(hr \times people)$	rate pathogens added to H	$lpha arphi_H$	[48]
	Pathogens/			5.403
$a_F$	$(hr \times people)$	rate pathogens added to $F$	$\alpha(1-\varphi_H)$	[48]
κ	1/people	fingertip to surface ratio	$\frac{6E-06}{\lambda}$	[18]

	ı			ı	Table A	1.4. No	de of I	Monday	y class s	schedu	le		
TW Room	1	2	3	4	5	6	7	8	9	10	11	12	13
1(102)	0	1	2	3	4	5	6	7	0	8	0	9	0
2(212)	10	11	0	12	0	13	0	14	15	16	17	18	19
3(202)	20	21	22	23	0	24	0	25	26	27	0	28	0
4(305)	29	30	31	32	33	34	0	0	0	35	36	37	38
5(210)	39	40	41	42	43	44	45	46	47	48	0	49	0
Table A.5. Node of Wednesday schedule													
TW Room	1	2	3	4	5	6	7	8	9	10	11	12	13
1(102)	0	1	2	3	4	5	6	7	0	8	0	9	10
2(212)	11	12	0	13	0	14	0	15	16	17	18	19	20
3(102)	21	22	23	24	0	25	0	26	27	28	0	29	0
					Tab	le A.6	. Node	of Frid	ay sche	dule			
TW Room	1	2	3	4	5	6	7	8	9	10	11	12	13
	0	1	2	2	1		-	7	0	0	0	0	10
1(102)	0	1	2	3	4	5	6	7 15	0	8	0	9	10
2(212)	11	12	0	13	0	14	0	15	16	17	18	19	20
3(102)	21	22	23	24	0	25	0	26	27	28	0	29	30
	Т			Tal	ole A.7.	Occuj	pancy o	of Mon	day cla	ss sche	dule		
TW Room	1	2	3	4	5	6	7	8	9	10	11	12	13
1(102)	108	0	0	0	0	0	0	0	140	0	189	0	61
2(212)	0	0	63	0	63	0	70	0	0	0	0	0	0
3(202)	0	0	0	0	103	0	72	0	0	0	82	0	48
4(305)	^						, 2	U	U	U	82	U	
\/	0	0	0	0	0	0	5	5	9	0	0	0	0
5(210)	0	0	0 0										
				0	0	0	5	5	9	0	0 20	0	0
				0	0	0	5	5	9	0	0 20	0	0
5(210)		0	0	0 0 Tabl	0 0 e A.8. 0	0 0 Occupa	5 0 ancy of	5 0 Wedne	9 0 esday cl	0 0 lass sci	0 20 nedule	0 0	0 7
5(210) TW Room	1	2	3	0 0 Tabl	0 0 e A.8. 0	0 0 Occupa 6	5 0 ancy of	5 0 Wedne	9 0 esday cl	0 0 lass scl	0 20 hedule	12	13
5(210) TW Room 1(102)	1 108	2 0	3 0	0 0 Tabl 4	0 0 e A.8. 0 5	0 0 Occupa 6	5 0 ancy of 7	5 0 Wedne 8	9 0 esday cl 9 140	0 0 lass scl 10	0 20 hedule 11 189	0 0 12	13
TW Room 1(102) 2(212)	1 108 0	2 0 0	3 0 63	0 0 Tabl 4 0 0	0 0 e A.8. 0 5 0 63	0 0 Occupa 6 0 0	5 0 ancy of 7 0 70 72	5 0 Wedno 8 0 0 0	9 0 esday cl 9 140 0	0 0 lass scl 10 0 0	0 20 nedule 11 189 0 82	12 0 0	13 0 0
TW Room 1(102) 2(212)	1 108 0	2 0 0	3 0 63	0 0 Tabl 4 0 0	0 0 e A.8. 0 5 0 63 103	0 0 Occupa 6 0 0	5 0 ancy of 7 0 70 72	5 0 Wedno 8 0 0 0	9 0 esday cl 9 140 0	0 0 lass scl 10 0 0	0 20 nedule 11 189 0 82	12 0 0	13 0 0
5(210) TW Room 1(102) 2(212) 3(102)	1 108 0 0	0 2 0 0 0	3 0 63 0	0 0 Tabl 4 0 0 0	0 0 e A.8. 0 5 0 63 103	0 0 0 0 0 0 0	5 0 ancy of 7 0 70 72	5 0 Wedno 8 0 0 0 0 of Fric	9 0 esday cl 9 140 0 0	0 0 0 lass scl 10 0 0 0	0 20 nedule 11 189 0 82	12 0 0 0	13 0 0 57
TW Room 1(102) 2(212) 3(102)	1 108 0 0	0 2 0 0 0	3 0 63 0	0 0 Tabl 4 0 0 0 0	0 0 e A.8. 0 5 0 63 103 able A.9	0 0 0 0 0 0 0 0 0. Occu	5 0 ancy of 7 0 70 72 upancy	5 0 Wedne 8 0 0 0 0 of Frice 8	9 0 esday cl 9 140 0 0 lay clas	0 0 0 10 0 0 0 0 s schee	0 20 nedule 11 189 0 82 lule	12 0 0 0 0	13 0 0 57
TW Room 1(102) 2(212) 3(102) TW Room 1(102)	1 108 0 0	0 2 0 0 0	3 0 63 0	0 0 Tabl 4 0 0 0 0	0 0 e A.8. 0 5 0 63 103 able A.9	0 0 0 0 0 0 0 0. Occu	5 0 ancy of 7 0 70 72 upancy 7	5 0 Wedne 8 0 0 0 0 of Frice 8	9 0 esday cl 9 140 0 0 lay clas 9	0 0 10 0 0 0 0 s sched	0 20 nedule 11 189 0 82 dule 11 189	0 0 12 0 0 0	13 0 0 57 13

Table A.10. Input parameters for influenza to the fomite-based transmission model[18]

Parameter	Units	Description	Values
	Pathogens/		
$\alpha$	$(hr \times people)$	Shedding rate	10000
ρ	/hr	Inoculation	15.8
$\mu_F$	/hr	Viral decay rate on F	0.121
$\mu_H$	/hr	Viral decay rate on H	88.2
		Viral transfer efficiency from <i>F</i> to	
$ au_{FH}$	proportion	H	0.1
		Viral transfer efficiency from <i>H</i> to	
$ au_{HF}$	proportion	F	0.025
$arphi_H$	proportion	Pathogen excreted to <i>H</i>	0.15
$\pi$	Unitless	Dose-response on mucosa	6.93E-05
	$1/(days \times$		
$ ho_{FH}$	people)	rate pathogens from $F$ to $H$	$ ho_T au_{FH}\kappa$
	$1/(days \times$		
$ ho_{HF}$	people)	rate pathogens from $H$ to $F$	$ ho_T au_{FH}$
	Pathogens/		
$a_H$	$(hr \times people)$	rate pathogens added to H	$\alpha \varphi_H$
	Pathogens/		$\alpha(1)$
$a_F$	$(hr \times people)$	rate pathogens added to F	$- arphi_H) \lambda$
			6E - 06
К	1/people	fingertip to surface ratio	λ

Table A.11. Input parameters for rhinovirus to the fomite-based transmission model[18]

Parameter	Units	Description	Values
	Pathogens/	•	
α	$(hr \times people)$	Shedding rate	1000
ρ	/hr	Inoculation	15.8
$\mu_F$	/hr	Viral decay rate on F	1.44
$\mu_H$	/hr	Viral decay rate on H	0.767
		Viral transfer efficiency from <i>F</i> to	
$ au_{FH}$	proportion	H	0.2
		Viral transfer efficiency from <i>H</i> to	
$ au_{HF}$	proportion	F	0.2
$\varphi_H$	proportion	Pathogen excreted to <i>H</i>	0.15
π	Unitless	Dose-response on mucosa	2.46E-03
	$1/(days \times$	-	
$ ho_{FH}$	people)	rate pathogens from $F$ to $H$	$ ho_T  au_{FH} \kappa$
	$1/(days \times$		
$ ho_{HF}$	people)	rate pathogens from $H$ to $F$	$ ho_T  au_{FH}$
	Pathogens/		
$a_H$	$(hr \times people)$	rate pathogens added to $H$	$\alpha \varphi_H$
_	Pathogens/		$\alpha(1)$
$a_F$	$(hr \times people)$	rate pathogens added to F	$-\varphi_H)\lambda$ $6E-06$
κ	1/people	fingertip to surface ratio	$\frac{0L-00}{1}$